Conformational Change of the Dimeric DsbC Molecule Induced by GdnHCl. A Study by Intrinsic Fluorescence†

Olga V. Stepanenko,‡ Irina M. Kuznetsova,‡ Konstantin K. Turoverov,*,‡ Chunjuan Huang,§ and Chih-chen Wang*,§

Institute of Cytology, Russian Academy of Science, Tihkoretsky av. 4, St. Petersburg 194064, Russia, and National Laboratory of Biomacromolecules, Institute of Biophysics, Chinese Academy of Sciences, 15 Datun Road, Beijing 100101, China

Received October 29, 2003; Revised Manuscript Received February 24, 2004

ABSTRACT: Unfolding−refolding of *Escherichia coli* DsbC, a homodimeric molecule, induced by GdnHCl was studied by intrinsic fluorescence. Interpretation of experimental fluorescence data was done together with the analysis of protein 3D structure. It is shown that although Cys 141 is the next neighbor of the single tryptophan residue (Trp 140), the sulfur atoms of the disulfide bond Cys 141−Cys 163 are far apart from the indole ring and cannot quench its fluorescence, while the potential quenchers are Met 136 and His 170. It was revealed that though each subunit of DsbC contains eight tyrosine residues, only three tyrosine residues (Tyr 171, Tyr 38, and Tyr 52) contribute to the bulk fluorescence of the molecule. The character of intrinsic fluorescence intensity changes induced by GdnHCl (equilibrium and kinetic data) and its parametric representation, the existence of an isosbestic point of fluorescence spectra at different GdnHCl concentrations, allowed suggesting a one-step character of DsbC denaturation and its reversibility.

How a polypeptide chain folds to a compact, highly ordered, and functional protein molecule is an important but not yet solved problem in protein science. The importance of protein folding has been strengthened by its close relationship with human health and biotechnology. The pathogenesis of many neurodegenerative diseases, such as Alzheimer's disease, Parkinson's disease, and Creutzfeldt−Jakob disease, has been recently characterized to correlate with aberrant protein folding that causes conformational rearrangement and the formation of amyloid fibril (*1*−*4*). The modern biotechnology would develop much faster than ever before if its bottleneck problem of inclusion body could be tackled efficiently using new knowledge of protein folding (*4*−*6*). The characterization of conformational changes and folding intermediates formed during the processes of protein unfolding−refolding is a powerful strategy to investigate protein folding. The majority of previous experiments of protein folding−unfolding were carried out on small single domain proteins; therefore, the folding−unfolding of large multidomain proteins are of great interest.

Escherichia coli DsbC is a soluble protein located in a periplasm with a main function of catalyzing the rearrangement of disulfide bonds and, therefore, is considered as a prokaryotic counterpart of the eukaryotic protein disulfide isomerase (PDI)[1] in endoplasmic reticulum (*7*, *8*). Like PDI, DsbC has been characterized to have intrinsic chaperone activity, which is even more pronounced than that of PDI in assisting in vitro protein folding (*9*). DsbC is a V-shaped molecule with each arm as a subunit, and each subunit consists of an N-terminal association domain and a C-terminal thioredoxin (Trx) domain connected by a hinged linker helix (*10*). The active sites in the Cys 98-Gly-Tyr-Cys 101 motif of both Trx domains of the dimeric DsbC molecule are essential for its isomerase activity, and only one active site is required for its oxidoreductase activity (*11*). By replacement of Cys with Ser, it has been shown that the active site disulfide bond is necessary for enzyme activity but not for chaperone activity, while the non-active site disulfide bond, Cys 141−Cys 163, plays an important role in folding, stability, and export of the molecule and its chaperone activity (*12*). Each subunit has only one tryptophan residue, Trp 140, close to the non-active site disulfide bond and eight tyrosine residues.

Intrinsic fluorescence has been widely used to investigate protein folding−unfolding and the properties of folding intermediates, because the fluorescence characteristics, such as spectrum, quantum yield, and anisotropy, are highly sensitive to the properties of the microenvironment of tryptophan and tyrosine residues in the protein macromolecule (*13*−*15*). In this work kinetic and equilibrium studies of unfolding and refolding of DsbC have been carried out by using different characteristics of its intrinsic fluorescence. The results showed that the guanidine hydrochloride (GdnHCl) induced denaturation of DsbC is a reversible two-state process.

MATERIALS AND METHODS

Materials. Expression vector pQE-30 and *E. coli* M15-(REP4) were from Qiagen, JM83 was from ATCC, dithio-

† This work was supported in part by RFBR-NSFC Grant 02-04-39009, INTAS Grant 2001-2347, Presidium of Russian Academy of Science Program "Physicochemical Biology", and the 973 Project from the Chinese Ministry of Science and Technology (G1999075608).

* To whom correspondence should be addressed. K.K.T.: fax, 7(812)247-0341; e-mail, kkt@mail.cytspb.rssi.ru. C.W.: phone, 8610-64888502; fax, 86-10-64872026; e-mail, chihwang@sun5.ibp.ac.cn.

‡ Russian Academy of Science.

§ Chinese Academy of Sciences.

[1] Abbreviations: PDI, protein disulfide isomerase; GdnHCl, guanidine hydrochloride; DTT, dithiothreitol.

10.1021/bi0359325 CCC: $27.50
Published on Web 04/10/2004

threitol (DTT) was from Serva, Tris-HCl was from AMRESCO, and molecular mass markers were from Bio-Rad.

The plasmid pDsbC, containing the full-length coding sequence of the DsbC precursor, was given generously by Dr. R. Glockshuber, Eidgenossische Technische Hochschule, Honggerberg, Switzerland. DsbC was prepared mainly according to Missiakas et al. (*12*, *16*). Transformed JM83-(REP4) strains containing the plasmid pQE-30 (DsbC) (*17*) were grown in LB media with 100 μg/mL ampicillin and 25 μg/mL kanamycin. The overnight culture was diluted 100-fold and incubated at 37 °C for 3 h followed by induction with isopropyl β-D-thiogalactopyranoside of 0.1 mM. Osmotic shock was used to release the soluble periplasmic proteins, which were dialyzed against buffer A (50 mM Tris-HCl, pH 8.0) and then loaded onto a Q-Sepharose fast-flow column (Amersham Pharmacia Biotech). After elution with a 0−0.4 M NaCl gradient in buffer A the fractions containing DsbC determined by SDS−15% polyacrylamide gel electrophoresis were collected, dialyzed against 50 mM NH_4HCO_3, and lyophilized. The concentration of DsbC was determined by measuring the absorbance at 280 nm using $A_{280nm}^{0.1\%} = 0.7$ (*7*).

The purified DsbC showed one band on SDS−15% polyacrylamide gel electrophoresis and thiol−protein reductase activity of 2.67×10^{-2} $\Delta A_{650nm}\cdot min^{-2}$ assayed by measuring the turbidity increase at 650 nm due to insulin reduction (*18*) and expressed as a ratio of the slope of a linear part of the turbidity curve to the lag time (*19*). Denatured DsbC was prepared by incubation of the protein of 0.5 mg/mL in GdnHCl at different concentrations at 4 °C for 24 h.

If not specified, 0.1 M Tris-HCl buffer, pH 7.5, was used in all experiments.

Fluorescence Measurements. All fluorescence experiments were carried out at 23 °C on a laboratory-made spectrofluorimeter with a thermostat (*20*). If not specified, fluorescence spectra were measured with excitation at 297 nm so that the contribution of tyrosine residues to the bulk protein fluorescence was neglected. The parameter $A = (I_{320}/I_{365})_{297}$ (I_{320} and I_{365} are fluorescence intensity at 320 and 365 nm, respectively) was used to characterize the fluorescence spectra (*20*). The fluorescence spectra and the values of parameter *A* were both corrected by the instrument sensitivity.

All kinetic experiments were performed in the microcells (101.016-QS 5 × 5 mm; Hellma, Germany). Denaturation of DsbC was carried out by injection of 350 μL of GdnHCl solution of appropriate concentrations into a cell containing 50 μL of native protein solution. Refolding of denatured DsbC was performed by injection of 350 μL of 0.75 M GdnHCl into a cell containing 50 μL of DsbC, which was previously denatured in 3.12 M GdnHCl at 4 °C for 24 h. The final concentration of GdnHCl was 1.05 M. In all experiments the final concentration of protein was 0.5 mg/mL. The fluorescence intensity at 320 and 365 nm was followed immediately for 10 min, and the final level was recorded overnight. The dead time determined with control experiments was less than 4 s (*21*).

Analysis of Protein 3D Structure. The location of tryptophan and tyrosine residues in the DsbC molecule was analyzed according to the atom coordinates of the crystal structure (file 1EEJ.ent in the PDB) (*10*, *22*). The microenvironment of a tryptophan or a tyrosine residue was determined as a set of atoms located in a distance less than r_0 from the geometrical center of the indole or phenol ring; r_0 was taken as 7 Å (*23*, *24*). The nearest atom in the microenvironment to each atom of the indole or phenol ring was specified, and the distance between them was determined. For tyrosine residues the neighbors of the OH group were also determined. The packing density of the atoms in the microenvironment was determined as a number of the atoms composing the microenvironment or as the part of the microenvironment volume (V_0) occupied by the atoms ($d = \sum V_i/V_0$). The volume occupied by each atom (V_i) was determined according to its van der Waals radius, and only the part inside the microenvironment was taken into account. The real values of atom volume are a little bit smaller as atoms are incorporated in chemical bonds. Nonetheless, it is insignificant for estimation of microenvironment packing density of tryptophan and tyrosine residues.

The efficiency of nonradiative energy transferred between any two chromophores was evaluated as follows (*25*):

$$W = \frac{1}{1 + \frac{2/3}{k^2}\left(\frac{R}{R_0}\right)^6} \quad (1)$$

Here R_0 is Förster distance, i.e., the averaged distance between a randomly orientated donor and acceptor at which $W = 0.5$, R is the distance between the geometrical centers of indole (or phenol) rings of a donor and an acceptor, and k^2 is the factor of mutual orientation of a donor and acceptor:

$$k^2 = (\cos\theta - 3\cos\theta_A \cos\theta_D)^2 \quad (2)$$

where θ is the angle between the directions of the emission oscillator of a donor and the absorption oscillator of an acceptor, θ_A is the angle between the emission oscillator and the vector connecting the geometrical center of the donor, and θ_D is the angle between the absorption oscillator and the vector connecting the geometrical center of the acceptor (*26*). The values of R_0 were taken from Eisenger et al. (*27*) and Steinberg (*28*). All other parameters were determined according to atom coordinates (*15*, *23*, *24*). Oscillators were considered to be rigid in all calculations.

RESULTS AND DISCUSSION

Microenvironment of the Tryptophan Residue. Each subunit of the DsbC molecule has only one tryptophan residue, Trp 140, which is located in the α-helix (Ser 130−Cys 141) of the C-terminal Trx-like domain just next to Cys 141 forming a disulfide bond with Cys 163 (Figure 1A). Two tryptophan residues in the molecule are more than 55 Å apart, and there is no energy transfer between them.

In each monomer of DsbC there are two disulfide bonds, Cys 98−Cys 101 and Cys 141−Cys 163. Sulfur atoms (SG) of disulfide bonds are known as effective quenchers of tryptophan fluorescence (*23*). As the sulfur atoms of Cys 98 and Cys 101 are 13.9 and 12.2 Å away from the center of the indole ring, respectively, they do not influence the tryptophan fluorescence. Cys 141 is a close neighbor of Trp 140 in the backbone. Nonetheless, as the side chains of the two neighbor residues are oriented in opposite directions from

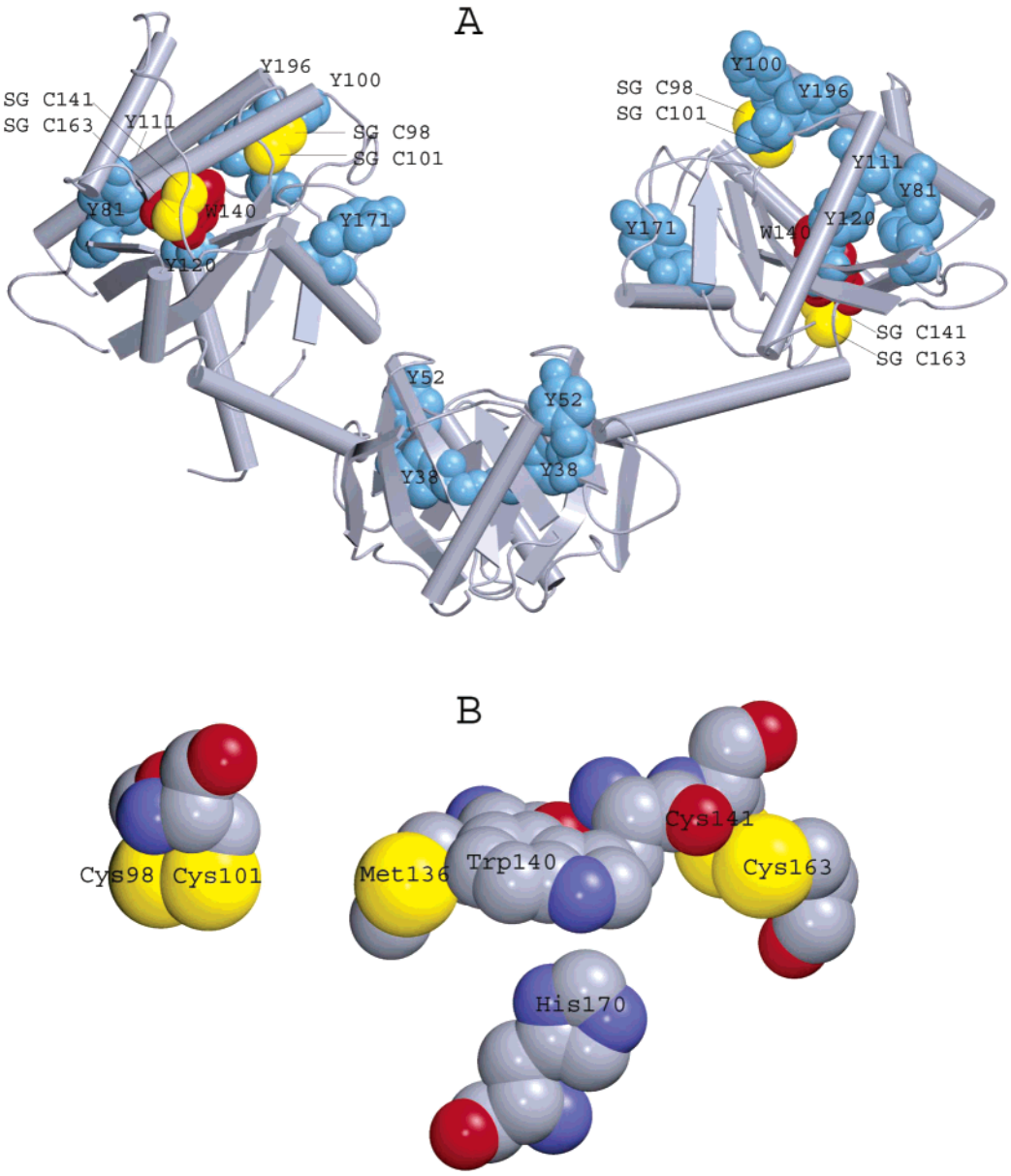

FIGURE 1: 3D structure of DsbC [file 1EEJ.ent from PDB (*10*, *22*)]. (A) Localization of tryptophan and tyrosine residues in the structure of DsbC. The backbone of the molecule is represented as a cartoon diagram; tryptophan (red) and tyrosine (blue) residues and sulfur atoms of disulfide bonds (yellow) are shown as solid van der Waals spheres. (B) Localization of the residues of Cys, Met, and His (potential quenchers of tryptophan fluorescence) in the vicinity of Trp 140. Graphic programs VMD (*29*) and Raster3D (*30*) were used.

the backbone, the distances between the sulfur atoms of disulfide bond Cys 141−Cys 163 and the indole ring of Trp 140 are 8.6 and 8.9 Å, respectively (Figure 1B). Therefore, none of the sulfur atoms of disulfide bonds quench tryptophan fluorescence of DsbC.

Potential quenchers of tryptophan fluorescence are Met 136 and His 170 (Figure 1B, Table 1), as the distance between the CZ3 atom of Trp 140 and the SD atom of Met 136 is only 4.10 Å, and the distances between the NE1 atom of Trp 140 and the ND1 and NE2 atoms of His 170 are 4.19 and 4.70 Å, respectively. The possible effects of the eight O atoms and eight N atoms of the peptide bonds in the microenvironments on the tryptophan fluorescence are not yet clear. There are no atoms of bound water in the close vicinity of Trp 140, while there are many side chains of nonpolar residues of Ile 79, Thr 94, Leu 121, Ala 122, Ile 139, Val 165, and Ile 167 and two aromatic rings of Tyr 120 and Phe 149 (Table 1). All in all, there are 82 atoms in the microenvironment of Trp 140 ($d = 0.80$). Thus the microenvironment of Trp 140 can be considered as hydrophobic, which accords to the blue fluorescence emission maximum at 312 nm (Figure 2).

Microenvironment of Tyrosine Residues. Each DsbC monomer contains eight tyrosine residues and one tryptophan residue. With excitation at 280 nm DsbC showed a fluorescence spectrum (Figure 2) with a maximum emission at 302 nm. Comparison of two fluorescence spectra excited at 280 and 297 nm, respectively, revealed that the parts in the red wavelength range are coincided but deviated significantly in the blue wavelength range. The difference spectrum presents the contribution of tyrosine residues to DsbC fluorescence excited at 280 nm.

To determine the contribution of each tyrosine residue in the bulk protein fluorescence, we examined their individual microenvironment, the energy transfer between tyrosine residues and from tyrosine residues to Trp 140. The

Table 1: Characteristics of the Trp 140 Microenvironment in *E. coli* DsbC[a]

residues in microenvironment		atoms	R^b (Å)
polar groups	Met 136	SD (CZ3)	4.10
	His 170	ND1 (NE1)	4.19
		NE2 (NE1)	4.70
nonpolar groups,	Ile 79	CB, CG1, CG2, **CD1**	3.60
rings of aromatic	Thr 94	**CG2**	4.45
residues and proline	Tyr 120	CB, CG, CD2	4.02
	Leu 121	CB, **CD2**	5.13
	Ala 122	CB	3.71
	Ile 139	CB, CG1, **CG2**, CD1	3.99
	Phe 149	CB, CG, CD2, **CE2**	4.06
	Val 165	CB, **CG1**	4.22
	Ile 167	CG1, **CD1**	4.40

[a] PDB code 1EEJ.ent. [b] *R* is the distance between S and N atoms of the polar groups and the nearest atom of the indole ring (given in parentheses) or the nearest atoms of the rings (given in bold).

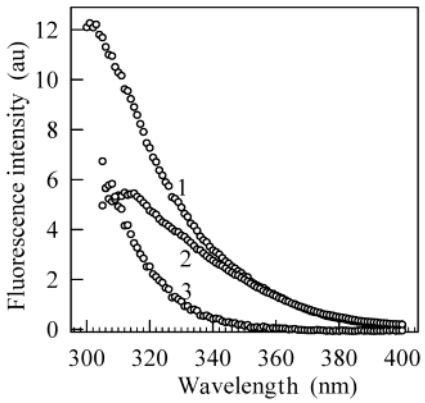

FIGURE 2: Fluorescence spectra of DsbC. Intrinsic fluorescence spectra of native DsbC with excitation at 280 nm (curve 1) and 297 nm (curve 2). Curve 3, the difference of subtracting curve 2 from curve 1, represents the fluorescence contribution of tyrosine residues.

microenvironment of tyrosine residues in the DsbC molecule differs significantly (Table 2). There are only 40 atoms in the microenvironment of Tyr 100; therefore, it is considered as external and accessible to solvent. In compliance with it many molecules of bound water were found in its microenvironment. In contrast, there are 77, 72, 79, and 79 atoms in the microenvironment of Tyr 38, Tyr 81, Tyr 111, and Tyr 120, respectively, and the microenvironment density of these residues is thus significantly higher. The fact that for all

Table 2: Characteristics of the Microenvironment of Tyrosine Residues in *E. coli* DsbC[a]

Tyr residue	N^b	amino acid side chains (potential quenchers of tyrosine fluorescence)			R_C (Å)	R_{OH} (Å)	oxygen atoms of bound water		
							N_{HOH}^c	R_C^d (Å)	R_{OH}^e (Å)
38	77 (73)	27	Met	SD	5.74		209	4.40	2.90
		51	Met	SD	4.56	4.51			
		61	Asn	OD1		6.04			
		66	Met	SD		6.77			
52	61 (41)	48	Gln	OE1	5.46	4.28	1	6.33	5.71
		48	Gln	NE2		4.18	90	6.74	5.61
		61	Asn	OD1	5.22	5.65	119	4.32	4.77
		61	Asn	ND2		4.09	126	6.10	5.59
81	72 (73)	105	His	ND1	4.66	4.54	12	6.49	
		105	His	NE2	4.71	3.77	63	6.25	
		112	Asn	OD1	6.44		93	6.16	6.17
		120	Tyr	OH		6.31	102	5.80	6.82
		146	Asn	OD1	5.41	5.31			
		146	Asn	ND2	3.49	4.11			
		150	Asp	OD1	4.47	2.99			
		150	Asp	OD2	5.38	4.02			
100	40 (22)	103	Lys	NZ	6.36	6.63	97	5.20	6.94
							138	4.12	2.67
							158	5.18	6.43
							169	5.39	4.67
							196	6.12	6.08
							201		5.12
111	79 (71)	107	Gln	OE1	6.31	5.61			
		107	Gln	NE2	5.70	4.43			
		196	Tyr	OH		4.61			
120	79 (72)	81	Tyr	OH		6.31	6	3.86	2.77
		105	His	ND1	4.35	2.86			
		105	His	NE2	6.05	4.93			
		108	Met	SD	5.95	5.01			
		153	Met	SD		6.88			
171	62 (47)						36	4.66	4.22
							107	6.43	5.10
							124	5.96	4.52
							131	4.16	2.64
196	68 (60)	103	Lys	NZ	6.87		99	4.39	3.03
		107	Gln	OE1	6.28	4.09	138	6.25	
		107	Gln	NE2	4.58	2.78	167	5.08	4.89
		111	Tyr	OH	4.56		169	6.02	5.97
		201	Glu	OE2		6.75	201	6.48	5.30

[a] PDB code 1EEJ.ent. [b] *N* is the number of atoms in the microenvironment of the tyrosine residue; the number of atoms in the microenvironment of the oxygen atom of the hydroxyl group of tyrosine is given in parentheses. [c] N_{HOH} is the number of molecules of bound water. [d] R_C is the distance from the geometrical center of the tyrosine residue. [e] R_{OH} is the distance from the oxygen atom of the hydroxyl group of the tyrosine residue.

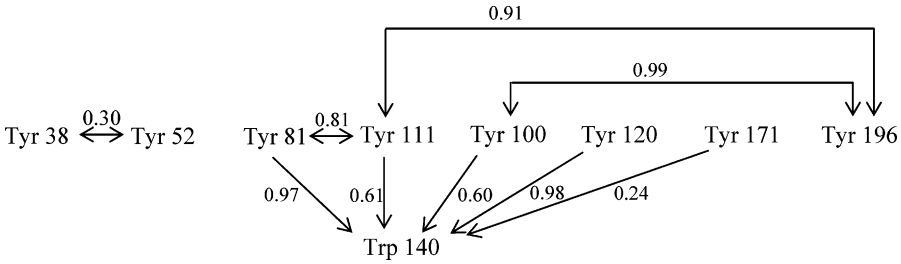

FIGURE 3: Efficiency of nonradiative energy transfer from tyrosine to tryptophan and between tyrosine residues in DsbC (1EEJ.ent, chain A).

tyrosine residues the number of the atoms in the microenvironment of oxygen atom of hydroxyl groups (Table 2, in parentheses) is less than that in the sphere with the geometrical center of phenol ring indicates that the hydroxyl groups of the tyrosine residues are all directed into the periphery of the molecule. It is particularly true for Tyr 52, Tyr 100, and Tyr 171, which are located near the surface of the molecule with low density of the microenvironment. Except for Tyr 100 and Tyr 171 there are numerous potential quenching groups in the microenvironment of the other six tyrosine residues, such as SD atoms of Met 27, Met 51, and Met 66 and oxygen atom OD1 of Asn 61 in the microenvironment of Tyr 38, and oxygen and nitrogen atoms of Gln 48 and Asn 61 in the microenvironment of Tyr 52. Nevertheless, the contributions of Tyr 38 and Tyr 52 may not be completely ignored.

As shown in Figure 3 there is efficient energy transfer from Tyr 81, Tyr 100, Tyr 111, and Tyr 120 to Trp 140 in the same C-terminal domain but not from the tyrosine residues located in the N-terminal domain. Also, there is no energy transfer between the tyrosine residues located in the different domains. Tyr 196 contributes little, if contributes at all, fluorescence for two reasons. First, there are many quenching groups in its microenvironment, such as Lys 102, Glu 201, and Gln 107, which the NE2 atom is in immediate contact with the OH group of Tyr 196. Second, energy from Tyr 196 can be transferred with high efficiency of 0.99 and 0.91 to Tyr 100 and Tyr 111, respectively, and further to Trp 140. As a result, only Tyr 171 makes a major contribution to the tyrosine fluorescence of the DsbC molecule.

GdnHCl-Induced Denaturation of DsbC: *Equilibrium Study*. Figure 4A shows that the fluorescence spectra of DsbC in GdnHCl at concentrations from 0.0 to 1.75 M have no change but are gradually red shifted when the GdnHCl concentration increases from 1.75 to 3.0 M and then remain unchanged with the GdnHCl concentration further increased to 6 M. The above suggested that DsbC basically retained its native conformation in GdnHCl at concentrations lower than 1.75 M. The conformation of DsbC changed with further increase of GdnHCl concentration and became completely unfolded in GdnHCl at concentrations higher than 3.0 M. There is an isosbestic point at 340 nm in the fluorescence spectra presented in comparative units (Figure 4B), suggesting a one-step conformational transition.

As shown in Figure 5A the fluorescence intensity at 320 nm of DsbC denatured in GdnHCl from 0.0 to 1.75 M did not change but abruptly decreased to 28% when the GdnHCl concentration increased to 3.0 M. Further increase of GdnHCl concentration had no effect on the fluorescence intensity (curve 1). In contrast, the fluorescence intensity at 365 nm

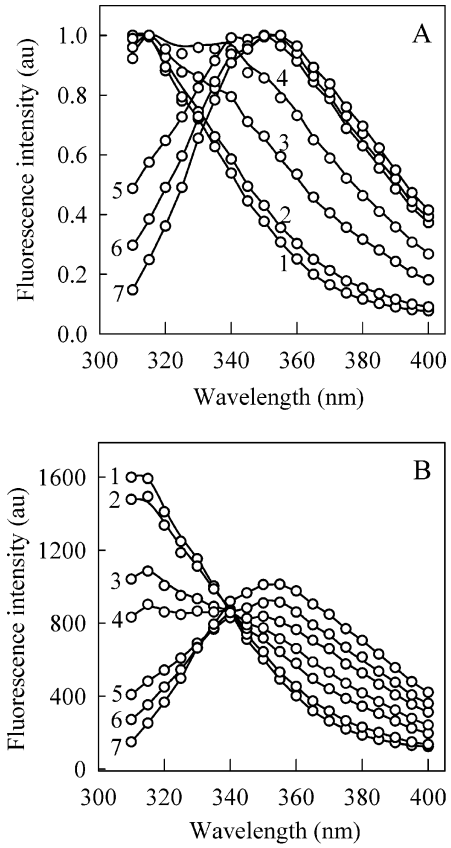

FIGURE 4: Fluorescence spectra of DsbC denatured in GdnHCl at different concentrations. Fluorescence spectra are normalized in their maxima (A) and in comparative units (B): curve 1, average fluorescence spectrum of DsbC in 0.0, 0.25, 0.50, 0.75, 1.00, 1.25, 1.50, and 1.75 M GdnHCl; curves 2−6, in GdnHCl at 2.0, 2.2, 2.4, 2.6, and 2.8 M, respectively; curve 7, an average fluorescence spectrum of DsbC in 3.0, 4.0, 5.0, and 6.0 M GdnHCl. $\lambda_{ex} = 297$ nm.

remained unchanged in GdnHCl concentrations from 0.0 to 1.75 M and jumped 3-fold with the increase of GdnHCl concentration to 3.0 M. Further increase of the concentration of GdnHCl had no effect on the fluorescence intensity (curve 2). The parameter *A* (Figure 5B) and the fluorescence anisotropy (Figure 5C) changed with GdnHCl concentrations in a similar way as the fluorescence intensity at 320 nm did.

GdnHCl-Induced Denaturation of DsbC: *Kinetics Study*. The time courses of the fluorescence intensity at 320 nm of DsbC denatured in different concentrations of GdnHCl are shown in Figure 6A. The kinetic curves in the presence of 0−1.75 M GdnHCl coincide with that for the native protein. In the range from 3.0 to 6.0 M GdnHCl the fluorescence intensity decreases to 28% of native protein fluorescence very rapidly. In the range from 1.75 to 3.0 M GdnHCl the

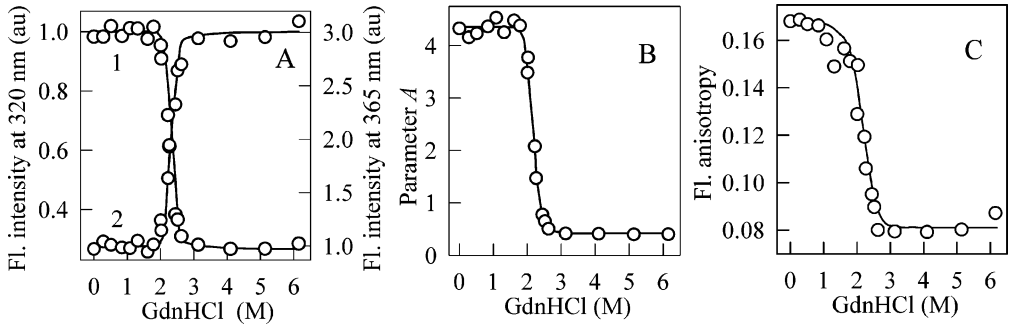

FIGURE 5: Denaturation of DsbC in GdnHCl monitored by tryptophan fluorescence. (A) Fluorescence intensity recorded at 320 (curve 1) and 365 nm (curve 2). (B) Parameter $A = I_{320}/I_{365}$. (C) Fluorescence anisotropy. $\lambda_{ex} = 297$ nm.

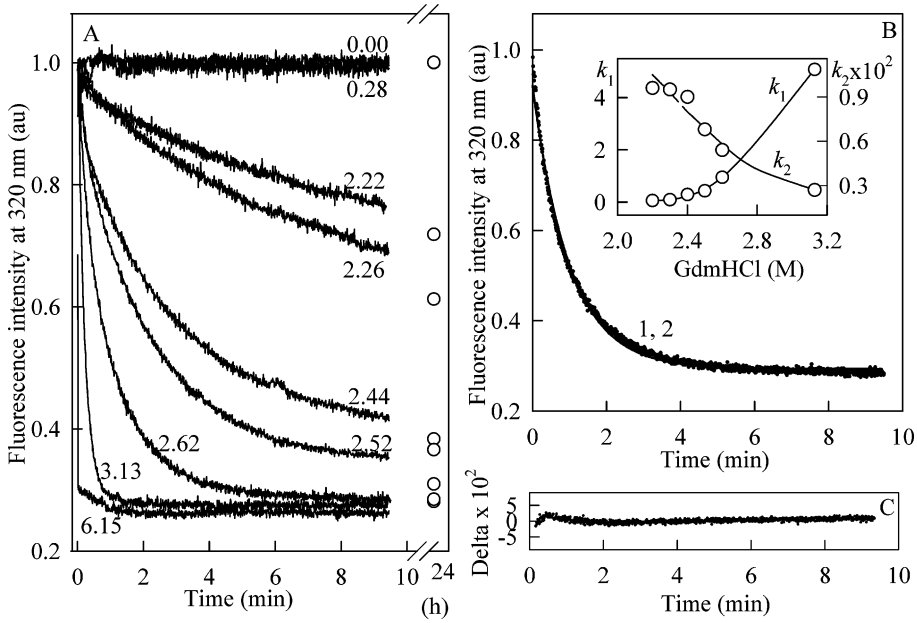

FIGURE 6: Time course of DsbC unfolding induced by GdnHCl. (A) The change of intrinsic fluorescence intensity of DsbC monitored at 320 nm. The values on the curves are the concentrations of GdnHCl. The protein concentration was 0.5 mg/mL; $\lambda_{ex} = 297$ nm. (B) Analysis of the kinetic curve of DsbC unfolding induced by 2.6 M GdnHCl. Curves 1 and 2: experimental decay curve (points) and calculated best fit of the fluorescence intensity that correspond to the values $k_1 = 0.949$ and $k_2 = 0.054$ s^{-1}, respectively. Insert: Dependence of the rate constants of DsbC denaturation k_i on GdnHCl concentration. (C) Deviation between the experimental and calculated curves. The protein concentration was 0.5 mg/mL.

fluorescence intensity decreases, tending to the value which is characteristic to equilibrium between native and unfolded states at the given GdnHCl concentration. The rate of achievement of the equilibrium state is gradually increased with the increase of GdnHCl concentration.

Analysis of the kinetic curves of DsbC denaturation was performed in the frame of a one-step transition:

$$\mathrm{N} \underset{k_2}{\overset{k_1}{\rightleftharpoons}} \mathrm{U} \tag{3}$$

Here, N is the native state, U is the unfolded state, and k_1 and k_2 are rate constants of the reactions. The relative fluorescence intensity $I(t)$ is determined as follows:

$$I(k_i,t) = I_0\left\{1 - \left(1 - \frac{I_U}{I_N}\right)\frac{k_1}{k_1 + k_2}(1 - \exp[-(k_1 + k_2)t])\right\} \tag{4}$$

where I_N and I_U are fluorescence intensities of the native and unfolded states, respectively, $I_U/I_N = 0.28$ (see above), and I_0 is fluorescence intensity at $t \rightarrow 0$. The values of the

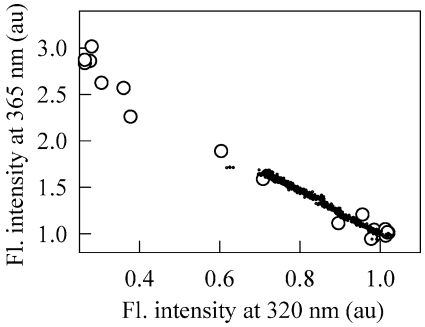

FIGURE 7: Parametric relationships between I_{320} and I_{365} nm characterizing DsbC unfolding induced by GdnHCl. The data were taken from the steady-state experiment (open circles; parameter is GdnHCl concentration) and from the kinetic experiment of DsbC denaturation by 2.4 M GdnHCl (black dots; parameter is the time interval from the unfolding initiation). $\lambda_{ex} = 297$ nm.

rate constants k_i were determined by the nonlinear least-squares method as the values that fit the minimum value:

$$\Phi = \sum_t [I_{exp}(t) - I(k_i,t)]^2 \tag{5}$$

Here, $I_{exp}(t)$ and $I(k_i,t)$ are experimental and calculated values

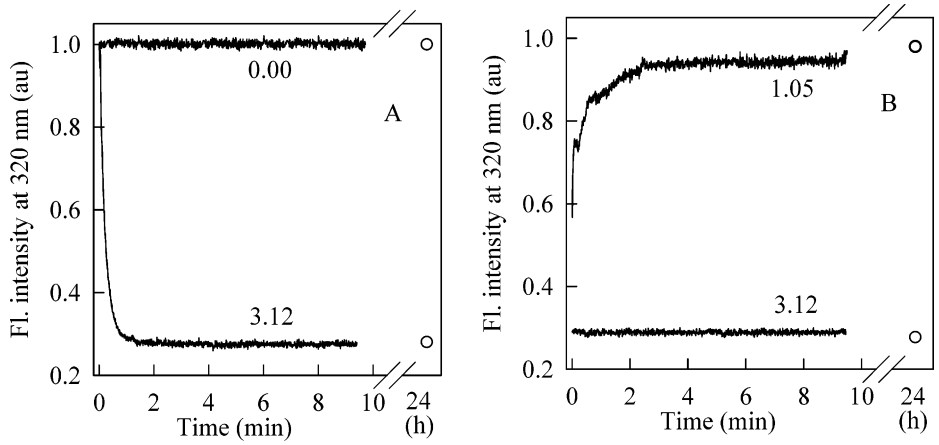

FIGURE 8: Kinetics of DsbC unfolding and refolding. (A) Unfolding of DsbC by GdnHCl. The final concentration of GdnHCl was 3.12 M. (B) Refolding of DsbC denatured in 3.12 M GdnHCl. The final concentration of GdnHCl was 1.05 M. Unfolding and refolding were initiated by an 8-fold dilution of protein solution by GdnHCl of appropriate concentration (3.57 and 0.75 M, respectively). The final concentration of the protein was 0.5 mg/mL.

of relative intensity, respectively. As an example Figure 6B shows the experimental kinetic curve, which reflects the time course of changes in fluorescence intensity, and the best theoretical fit within the frame of the model (eq 3), both for the final GdnHCl concentration of 2.6 M. The best fit of the experimental data was achieved when $k_1 = 0.949$ and $k_2 = 0.054\ s^{-1}$. Figure 6C shows that the residuals are of statistical character. The proximity of χ^2 [$\chi^2 = \Phi/(n - p)$, where n is the number of experimental points and p is the number of examined parameters] to the unity ($\chi^2 = 1.12$) and the randomness of the residuals prove the validity of the chosen kinetic model. The dependencies of the values of constants k_i on the GdnHCl concentration are given in Figure 6 (insert).

Parametric Relationship between Two Independent Extensive Characteristics of the System as an Approach for Protein Folding−Unfolding Examination. Any extensive characteristic of a system consisting of two components is determined by the simple equation:

$$I(\theta) = \alpha_1(\theta)I_1 + \alpha_2(\theta)I_2 \tag{6}$$

where I_1 and I_2 are the values of $I(\theta)$ at 100% content of the first and the second component, respectively, and $\alpha_1(\theta) \neq \alpha_2(\theta)$ are the relative fraction of these components in the system, $\alpha_1(\theta) + \alpha_2(\theta) = 1$; θ is any parameter depending on which content of the components is changed. Denaturant concentration, temperature, pH of the solution, etc. can be taken as a parameter. Only for extensive characteristics which give quantitative characterization of the system is eq 6 valid, and the fraction of the components in the system, as well as the equilibrium constant K, can be determined by simple equations:

$$\alpha_1(\theta) = \frac{I(\theta) - I_2}{I_1 - I_2} \quad \alpha_2(\theta) = \frac{I_1 - I(\theta)}{I_1 - I_2} \quad K(\theta) = \frac{I_1 - I(\theta)}{I(\theta) - I_2} \tag{7}$$

If intensive characteristics [such as fluorescence spectrum position, parameter A (*20*), and fluorescence anisotropy, which characterize the system qualitatively] are used, these equations for determination of $\alpha_1(\theta)$, $\alpha_2(\theta)$, and $K(\theta)$ are not valid (*13*), though often no account is taken of this in the investigations of protein conformation transition. For any two independent extensive characteristics we have

$$I_1(\theta) = \alpha_1(\theta)I_{1,1} + \alpha_2(\theta)I_{2,1} \tag{8}$$

and

$$I_2(\theta) = \alpha_1(\theta)I_{1,2} + \alpha_2(\theta)I_{2,2} \tag{9}$$

Eliminating $\alpha_1(\theta)$ and $\alpha_2(\theta)$ from eqs 8 and 9, we can obtain the relationship between $I_1(\theta)$ and $I_2(\theta)$:

$$I_1(\theta) = a + bI_2(\theta) \tag{10}$$

where $a = I_{1,1} - [(I_{2,1} - I_{1,1})/(I_{2,2} - I_{1,2})]I_{1,2}$ and $b = (I_{2,1} - I_{1,1})/(I_{2,2} - I_{1,2})$.

Equation 10 means that if with the change of parameter θ the transition between states 1 and 2 follows the model "all or none" without formation of the intermediate states, then the parametric relationship between any two extensive characteristics must be linear. If the experimentally recorded parametric relationship between two extensive characteristics of the system is not linear, it unequivocally means that the process of transition from the initial to the final state is not a one-stage process but it proceeds with the formation of one or several intermediate states. This approach has been used for characterization of intermediate states of carbonic anhydrase II (*31*), creatin kinase (*32*), and actin (*15*, *21*) in our laboratory and is also widely used in other laboratories (*33*).

The parametric relationship between fluorescence intensities recorded on the different slopes of the fluorescence spectrum (I_{320} and I_{365}) was constructed. The GdnHCl concentration and time of protein denaturation induced by 2.4 M GdnHCl were taken as a parameter. Both parametric curves obtained were well approximated by a straight line, and it was revealed that they coincide (Figure 7).

Renaturation of Denatured DsbC: Kinetics Study. As shown in Figure 8 the fluorescence intensity of DsbC denatured in 3.12 M GdnHCl rapidly increased and reached the level for native protein in 2−3 min on GdnHCl concentration decrease from 3.12 to 1.05 M. It is shown that fluorescence spectra of native protein transferred to 1.0 M

GdnHCl and that of protein transferred from 3.0 to 1.0 M GdnHCl are coincident.

CONCLUSIONS

The above results indicate that GdnHCl-induced denaturation of DsbC is an all or none process; i.e., protein exists only in two states, native and completely unfolded. The native state is characterized by a blue fluorescence spectrum position ($\lambda_{max} = 331$ nm at $\lambda_{ex} = 297$ nm), a high value of parameter $A = 4.3$, and resistance to GdnHCl up to 1.75 M. When the GdnHCl concentration is changed from 1.75 to 3.0 M, parameter A decreases dramatically from 4.3 to 0.4. Completely unfolded DsbC has a red fluorescence spectrum ($\lambda_{max} = 360$ nm at $\lambda_{ex} = 297$ nm), which is typical for many proteins in the unfolded state. Fluorescence anisotropy constancy in the range of 0−1.75 M GdnHCl suggests that DsbC remains in dimeric form in GdnHCl until 1.75 M and dissociates synchronously with monomer unfolding when GdnHCl concentration further increases.

The facts that the character of the parametric plot of the relation between I_{320} and I_{365} with concentration of GdnHCl or time in the course of denaturation taken as the parameter is linear and that the fluorescence spectra of the protein in different GdnHCl concentrations have an isosbestic point confirm the one-step character of DsbC denaturation. Furthermore, the increase of fluorescence intensity in the refolding process of DsbC from 3.0 to 1.0 M GdnHCl and coincidence of fluorescence spectra of DsbC in 1.0 M GdnHCl obtained as a result of protein denaturation or renaturation showed a reversible character of DsbC denaturation.

REFERENCES

1. Carrell, R. W., and Gooptu, B. (1998) Conformational changes and disease−serpins, prions and Alzheimer's, *Curr. Opin. Struct. Biol. 8*, 799−809.
2. Harper, J. D., and Lansbury, P. T., Jr. (1997) Models of amyloid seeding in Alzheimer's disease and scrapie: mechanistic truths and physiological consequences of the time-dependent solubility of amyloid proteins, *Annu. Rev. Biochem. 66*, 385−407.
3. Uversky, V. N., Talapatra, A., Gillespie, J. R., and Fink, A. L. (1999) Protein deposits as the molecular basis of amyloidosis, *Med. Sci. Monitor 5*, 1001−1012, 1238−1254.
4. Fink, A. L. (1998) Protein aggregation: folding aggregates, inclusion bodies and amyloid, *Folding Des. 3*, R9−R23.
5. Wetzel, R. (1994) Mutations and off-pathway aggregation of proteins, *Trends Biotechnol. 12*, 193−198.
6. Speed, M. A., Wang, D. I., and King, J. (1996) Specific aggregation of partially folded polypeptide chains: the molecular basis of inclusion body composition, *Nat. Biotechnol. 14*, 1283−1287.
7. Hiniker, A., and Bardwell, C. A. (2003) Disulfide bond isomerization in prokaryotes, *Biochemistry 42*, 1179−1185.
8. Zapun, A., Missiakas, D., Raina, S., and Creighton, T. E. (1995) Structural and functional characterization of DsbC, a protein involved in disulfide bond formation in *Escherichia coli*, *Biochemistry 34*, 5075−5089.
9. Chen, J., Song, J. L., Zhang, S., Wang, Y., Cui, D. F., and Wang, C. C. (1999) Chaperone activity of DsbC, *J. Biol. Chem. 274*, 19601−19605.
10. McCarthy, A. A., Haebel, P. W., Torronen, A., Rybin, V., Baker, E. N., and Metcalf, P. (2000) Crystal structure of the protein disulfide bond isomerase, DsbC, from *Escherichia coli*, *Nat. Struct. Biol. 7*, 196−199.
11. Sun, X. X., and Wang, C. C. (2000) The N-terminal sequence (residues 1−65) is essential for dimerization, activities, and peptide binding of *Escherichia coli* DsbC, *J. Biol. Chem. 275*, 22743−22749.
12. Liu, X. Q., and Wang, C. C. (2001) Disulphide-dependent folding and export of *Escherichia coli*. DsbC, *J. Biol. Chem. 276*, 1146−1151.
13. Eftink, M. R. (1994) The use of fluorescence methods to monitor unfolding transitions in proteins, *Biophys. J. 66*, 482−501.
14. Turoverov, K. K., Verkhusha, V. V., Shavlovsky, M. M., Biktashev, A. G., Povarova, O. I., and Kuznetsova, I. M. (2002) Kinetics of actin unfolding induced by guanidine hydrochloride, *Biochemistry 41*, 1014−1019.
15. Turoverov, K. K., and Kuznetsova, I. M. (2003) Intrinsic fluorescence of actin, *J. Fluoresc. 13*, 41−57.
16. Missiakas, D., Georgopoulos C., and Raina, S. (1994) The *Escherichia coli*. dsbc (xprA) gene encodes a periplasmic protein involved in disulphide bond formation, *EMBO J. 13*, 2013−2020.
17. Liu, X.-Q., Zhang, S., Pan, X.-M., and Wang, C.-C. (1999) A novel method of increasing production of mature proteins in the periplasm of *Escherichia coli*, *Protein Sci. 8*, 2085−2089.
18. Holmgren, A. (1979) Thioredoxin catalyzes the reduction of insulin disulfides by dithiothreitol and dihydrolipoamide, *J. Biol. Chem. 254*, 9627−9632.
19. Martínez-Galisteo, E., Padilla, C. A., Garcia-Alfonso, C., López-Barea, J., and Barcena, J. A. (1993) Purification and properties of bovine thioredoxin system, *Biochimie 75*, 803−809.
20. Turoverov, K. K., Biktashev, A. G., Dorofeyuk, A. S., and Kuznetsova, I. M. (1998) Devices and programs for investigation of spectral, polarizational and kinetic characteristics of fluorescence in solution, *Tsitologiia 40*, 806−817.
21. Kuznetsova, I. M., Stepanenko, O. V., Stepanenko, O. V., Povarova, O. I., Biktashev, A. G., Verkhusha, V. V., Shavlovsky, M. M., and Turoverov, K. K. (2002) The place of inactivated actin and its kinetic predecessor in actin folding-unfolding, *Biochemistry 41*, 13127−13132.
22. Bernstein, F. C., Koetzle, T. F., Williams, G. J. B., Meyer, E. F., Jr., Brice, M. D., Rodgers, J. R., Kennard, O., Shimanouchi, T., and Tasumi, M. (1977) The Protein Data Bank: a computer-based archival file for macromolecular structures, *J. Mol. Biol. 112*, 535−542.
23. Kuznetsova, I. M., and Turoverov, K. K. (1998) What determines characteristics of protein intrinsic UV-fluorescence? Analysis of properties of microenvironment and peculiarities of localization of tryptophan residues in proteins, *Tsitologia 40*, 747−762.
24. Turoverov, K. K., Kuznetsova, I. M., and Zaitzev, V. N. (1985) The environment of the tryptophan residue in pseudomonas aeruginosa azurin and its fluorecsence properties, *Biophys. Chem. 23*, 79−89.
25. Forster, Th. (1960) Transfer mechanisms of electronic excitation energy, *Radiat. Res., Suppl. 2*, 326−339.
26. Dale, R. E., and Eisinger, J. (1974) Intramolecular distances determined by energy transfer. Dependence on orientational freedom of donor and acceptor, *Biopolymers 13*, 1573−1605.
27. Eisinger, J., Feuer, B., and Lamola, A. A. (1969) Intramolecular singlet excitation transfer. Applications to polypeptides, *Biochemistry 8*, 3908−3915.
28. Steinberg, I. Z. (1971) Long-range nonradiative transfer of electronic excitation energy in proteins and polypeptides, *Annu. Rev. Biochem. 40*, 83−114.
29. Humphrey, W., Dalke, A., and Schulten, K. (1996) VMD: visual molecular dynamics, *J. Mol. Graphics 14*, 33−38.
30. Merritt, E. A., and Bacon, D. J. (1977) Raster3D: Photorealistic molecular graphics, *Methods Enzymol. 277*, 505−524.
31. Bushmarina, N. A., Kuznetsova, I. M., Biktashev, A. G., Turoverov, K. K., and Uversky, V. N. (2001) Partially folded conformations in the folding pathway of bovine carbonic anhydrase II: a fluorescence spectroscopic analysis, *ChemBioChem 2*, 813−821.
32. Kuznetsova, I. M., Stepanenko, O. V., Turoverov, K. K., Zhu, L., Zhou, J.-M., Fink, A. L., and Uversky, V. N. (2002) Unraveling multistate unfolding of rabbit muscle creatine kinase, *Biochim. Biophys. Acta 1596*, 138−155.
33. Kuznetsova, I. M., Turoverov, K. K., and Uversky, V. N. (2004) Use of the phase diagram method to analyze the protein unfolding-refolding reactions: fishing out the "invisible" intermediates, *J. Proteome Res. 3*, 000−000.

BI0359325